JOURNAL OF MOLECULAR SPECTROSCOPY 163, 541–558 (1994)

The Dalby System of Iodine Revisited: Rotationally Resolved (2 + 1) REMPI Spectra of the Rydberg State $[^2\Pi_{1/2}]_c6s;1g$ of I_2

ÁGÚST KVARAN, HUASHENG WANG, AND JÓN ÁSGEIRSSON

Science Institute, University of Iceland, Dunhaga 3, 107 Reykjavík, Iceland

Partly rotationally resolved (2 + 1) resonance-enhanced multiphoton ionization spectra of the vibrational bands in the Dalby system ($[^2\Pi_{1/2}]_c6s;1g \leftarrow X$) of $I_2(g)$ have been recorded and analyzed at room temperature. The simulation technique used in spectral analyses is described and discussed. A statistical weight ratio of odd total nuclear spin: even total nuclear spin = 7:5 is clearly seen from the same relative intensities for rotational lines corresponding to odd J'':even J'' transitions. Rotational constants ($B_{v'}$ and $D_{v'}$) and corresponding internuclear distances ($r_{v'}$) for the Rydberg state ($[^2\Pi_{1/2}]_c6s;1g$) are obtained, as well as the characteristic rotational parameters $B'_e = 0.04036 \pm 0.00001$ cm^{-1}, $\alpha'_e = (1.12 \pm 0.02) \times 10^{-4}$ cm^{-1}, and $r'_e = 2.5656 \pm 0.0005$ Å. Vibrational analyses based on determination of band origins from the spectral simulations were performed to obtain $\omega_e = 241.8 \pm 0.5$ cm^{-1} and $\omega_e x_e = 0.64 \pm 0.07$ cm^{-1}, in good agreement with earlier results by Dalby *et al.* (*Can. J. Phys.* **55**, 1033–1046, 1977).

INTRODUCTION

Increasing use of multiphoton optical absorption measurements has made studies of atomic and molecular electronic states, not easily accessible by standard one-photon absorption, more feasible. This can be due to either different selection rules or differences in accessibility due to technical reasons. Thus, for example, excited states of homonuclear diatomic molecules of the same parity as those in the ground state can be accessed with an even number of photons excitation.

For I_2, over 40 ungerade Rydberg states in which the molecules have a $[^2\Pi_{3/2}]$ or $[^2\Pi_{1/2}]$ core of g symmetry, and the Rydberg electrons are in *np* or *nf* orbitals, have been identified from high-resolution vacuum-ultraviolet absorption spectra (*1*). Only 7 Rydberg states of g symmetry were identified this way, however, and for several of these the analyses are controversial.

By use of (2 + 1) resonance-enhanced multiphoton ionization (REMPI) a total of 20 gerade Rydberg states for iodine, in which the molecules also have $[^2\Pi_{3/2g}]$ or $[^2\Pi_{1/2g}]$ cores but the Rydberg electrons are in *ns* or *nd* orbitals, have been characterized (*2–8*). Dalby *et al.* reported the first (2 + 1) REMPI system in iodine vapor with a band origin (T_e) at 53 563 cm^{-1}, assigning it to the gerade Rydberg state, $[^2\Pi_{1/2g}]_c6s;1g$ (Dalby system) (*2, 3*). Lehmann *et al.* (*4*) assigned a system with an origin at 48 426 cm^{-1}, found in iodine vapor, to the spin-orbit-split companion to the Dalby system, $[^2\Pi_{3/2}]_c6s;2g$ (Goodman system). A total of five systems were observed by Miller for jet-cooled iodine or iodine vapor at room temperature (*5*), one of which has a band origin at 52 994 cm^{-1} and was tentatively assigned to $[^2\Pi g]_c n\sigma;0g$. The band origin for one of the other four systems was later suggested to be at 56 577 cm^{-1} (*6*). Wu and Johnson reported and assigned four high-lying Rydberg states at 62 440 ($[^2\Pi_{3/2}]_c5d;0g$), 68 335, 68 407, and 68 434 cm^{-1} ($[^2\Pi_{3/2}]_c6d;0g$, 1g, and 2g, respectively) (*6*). Some of the above mentioned assignments have turned out to be

0022-2852/94 $6.00

controversial. Thus Dasari and Dalby reassigned the Goodman system as being due to transition to the $[^2\Pi_{3/2}]_c6s;1g$ state and predicted the $[^2\Pi_{3/2}]_c6s;2g$ state origin to be near 47 931 cm^{-1} (*7*). Recently Donovan *et al.* published an extensive work on the overall (2 + 1) REMPI spectrum for I_2, reassigning some previously observed gerade Rydberg states and reporting a total of 12 new band systems in the two-photon energy region 48 000–75 300 cm^{-1} (*8*).

Assignment of the gerade Rydberg states largely has been based on analyses of the vibrational structure of the spectral systems and positions of band origins. Characteristically, vibrational level spacing in the excited Rydberg states is found to be about 5–15% larger than that for the ground state. Therefore hot bands normally can be distinguished easily from $v'' = 0$ transitions and thus band origins determined. Quantum defect values, δ, for an electron in a particular Rydberg orbital then can be calculated from

$$T_0([\Omega_c]nl) = \mathrm{IP}(\Omega_c) - \frac{R_\infty}{[n - \delta(])]^2}, \tag{1}$$

where $T_0([\Omega_c)nl)$ is the observed molecular electronic term value, R_∞ is the Rydberg constant, and $\mathrm{IP}(\Omega_c)$ is the ionization potential to the molecular ions ($[^2\Pi_{3/2g}]$ or $[^2\Pi_{1/2g}]$) to which the series converges (*9, 10*). Assignment of states involved can be made from the fact that δ is found to be virtually the same when the orbital is associated with a molecular core as when associated with an atomic core (*8*). Furthermore, the energy spacing between $[^2\Pi_{3/2}]ns;2g$ and $[^2\Pi_{1/2}]ns;0g$ pairs on one hand, and between $[^2\Pi_{3/2}]ns;1g$ and $[^2\Pi_{1/2}]ns;1g$ pairs on the other hand, should be close to that of the two Ω_c states of the positive ions (*8*). Precise splitting between the two $\Omega_c = {}^1/_2$ states ($\Omega = 0$ and 1) and the two $\Omega_c = {}^3/_2$ states ($\Omega = 1$ and 2), however, can not easily be predicted (*8, 11, 12*).

Intensity alterations of the spectral systems as the polarity of the excitation light is changed between being linear (LP) and circular (CP) have been made use of for helping distinguish between $\Omega = 0$ states and $\Omega = 1$ or 2 states (*3, 8*). The predicted ratio of the two-photon transition probability for photons linearly polarized to that for photons circularly polarized is ${}^2/_3$ for $0_g^+ \rightarrow 1g$, 2g transitions but ranges from ∞ to ${}^3/_2$ for $0_g^+ \rightarrow 0_g^+$ transitions (*13, 14*). While in a number of cases intensities have been found to change according to these predictions, unexpected intensity variations (ratios < 0.1) have been found above 62 000 cm^{-1} (two-photon energies) for a number of systems which are believed to correspond to $\Omega = 1$ excited states. This effect has been explained as being due to predissociation (*8*), but it is well known that such processes take place in MPI experiments of iodine (*15–18*).

More explicit assignments and analyses of the excited states by virtue of rotational analyses of vibrational bands of the (2 + 1) REMPI spectra have been made only to a limited extent (*3, 8, 19*). Dalby *et al.* determined the Ω value of the upper state in the Dalby system ($[^2\Pi_{1/2g}]_c6s;1g$) from the shape of the bandhead of a medium-resolution spectrum of the ($v' = 0$, $v'' = 0$) band which showed clearly resolved *O* and *P* heads with characteristic relative intensities as expected for $0_g^+ \rightarrow 1g$ transitions (*3*). Donovan *et al.* also made use of bandhead shapes, along with analyses based on determining quantum defect values as well as measurements of polarization ratios, in order to assign Rydberg states (*8*). Recently Wang *et al.* published a brief note on simulation analyses of the ($v' = 0$, $v'' = 1$) band in the Dalby system and determined corresponding rotational constants ($B_{v'=0}$ and $D_{v'=0}$) (*19*).

Our ultimate goal in subsequent publications will be to analyze high-resolution rotational REMPI spectra of halogen-containing compounds in order to obtain information on rotational parameters of the Rydberg states involved, and to understand curve crossing and predissociation mechanisms from observed perturbations in the spectra (*8*). In this publication, we present a detailed analysis of rotational contours for the (2 + 1) REMPI spectrum in the single-photon spectral region 26 300–27 600 cm^{-1} (two-photon spectral region, 52 600–55 200 cm^{-1}) for iodine. We demonstrate the simulation analyses procedure and emphasize analyses of the excited state in the Dalby system ($[^2\Pi_{1/2}]_c 6s;1g$) to derive rotational as well as vibrational spectroscopic parameters.

EXPERIMENTAL DETAILS

The experimental arrangement for recording REMPI spectra for iodine is shown schematically in Fig. 1. Tunable UV laser pulses were generated by a Lumonics Hyperdye 300 laser pumped by a Lumonics 510 excimer laser. The wavelength range 362–380 nm was covered by using the dye BPBD366. The pulses from the dye laser were reflected 90 degrees by a Pellin Broca prism and focused by a 20-cm-focal-length lens into a simple glass ionization cell fitted with stainless steel electrodes (20-mm diameter and about 20 mm apart) which were typically kept at ±90 V by batteries. The cell contained vapor pressure of iodine at room temperature. Current pulses due to ionization were picked up at the electrodes and amplified by a balanced bias differential amplifier suitable for detection of laser-induced multiphoton ionization (*20*). Due to a delay difference between the pulses from the two electrodes, the pulse signal from the differential amplifier sometimes showed two maxima. The signal was

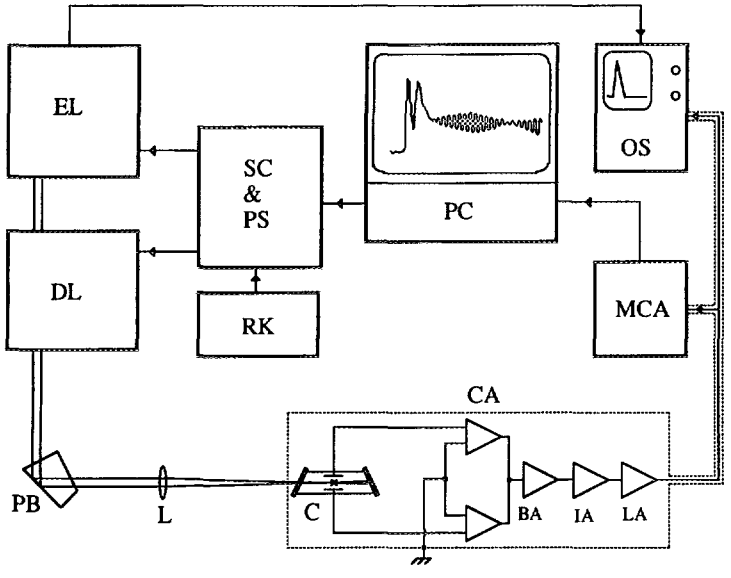

FIG. 1. Schematic figure of the apparatus used. EL, excimer laser (Lumonics 510); DL, dye laser (Hyperdye-300); PB, Pellin Broca prism; L, 20-cm focal lens; C, sample cell/ionization cell; CA, current amplifier; BA, balanced bias differential current amplifier; IA, integrator; LA, linear amplifier; MCA, multichannel analyzer; PC, IBM PC/XT 286 computer; OS, oscilloscope (V-422); SC, scan control unit; PS, power supply; RK, remote keypad.

therefore integrated by a conventional integration circuit and fed through a linear amplifier before entering a homemade multichannel analyzer for voltage peak height measurement and recording. Typically the total amplifying gain was about 10^5. A common earth connection for the electronic circuits and an aluminum foil shielding for the cell/electrodes was found to be important in order to avoid picking up noise from the surroundings. Averaged pulse heights for a fixed sampling time were recorded and displayed as a function of excitation frequency (ν_{exc}/cm^{-1}) (REMPI spectra) on an IBM/XT 286 computer. The various equipment units could be controlled either by the computer or by specific laser control units as shown in Fig. 1.

Typically the laser was run at a 20-Hz repetition rate, and a pulse sampling time of 5 sec was used to average 100 pulses for each measurement. The bandwidth of the laser beam was about 0.05 cm^{-1}. Care was taken to prevent power broadening due to ac Starck effects by minimizing laser power. The gatewidth of the multichannel analyzer was set at about 10 msec and the threshold was adjusted to minimize reading of low-voltage pulses due to noise. The dye laser output was scanned in wavenumber steps, typically 0.5 cm^{-1} steps for low-resolution (overall) spectra but 0.02–0.05 cm^{-1} steps for high-resolution (rotational contours) spectra.

Calibration of the dye laser wavelength over the visible and UV region was achieved by recording the neon signal from an optogalvanic cell (visible region) and the REMPI signal from iodine atomic lines (UV region) (*8, 21*). The accuracy of the calibration in the spectral region studied here was found to be ± 1 cm^{-1}.

RESULTS AND DATA ANALYSES

(a) (2 + 1) REMPI Spectra

Figure 2 shows an overall (2 + 1) REMPI spectrum of the Dalby system due to two-photon resonance excitation from the ground state to the Rydberg state

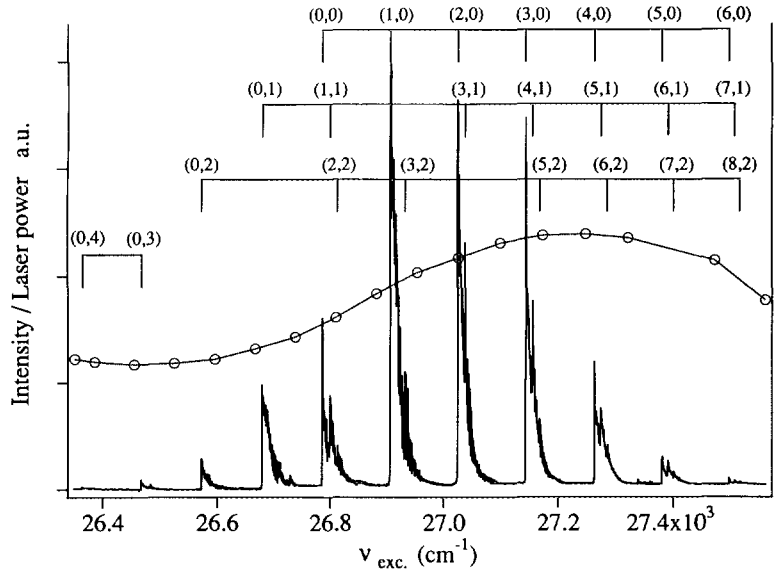

FIG. 2. (2 + 1) REMPI spectrum of the Dalby system, $[^2\Pi_{1/2}]_c 6s;1g \leftarrow X$, for iodine: current vs laser excitation frequency (in wavenumbers). Vibrational quantum numbers (v', v'') of bands are indicated. The circles and dotted curve show the relative laser power.

$[^2\Pi_{1/2}]_c 6s;1g$, followed by a single-photon ionization. Peaks represent vibrational bands as indicated. The spectrum has not been corrected for variation in laser power with wavenumber, which is shown in the same figure. Rotational contours of the vibrational bands are shown in Fig. 3 plotted on a relative excitation wavenumber scale ($\Delta\nu_{exc}$/ cm^{-1}). The vibrational bands show clearly resolved *O* and *P* heads (*3, 8, 19*) with blue degraded band contours. The spacing between *O* and *P* peaks increases with v' but decreases with v'' (Fig. 4). Characteristically regular alterations in peak intensities and beat structure due to overlapping *O*, *P*, (*Q*), *R*, and *S* rotational lines are seen

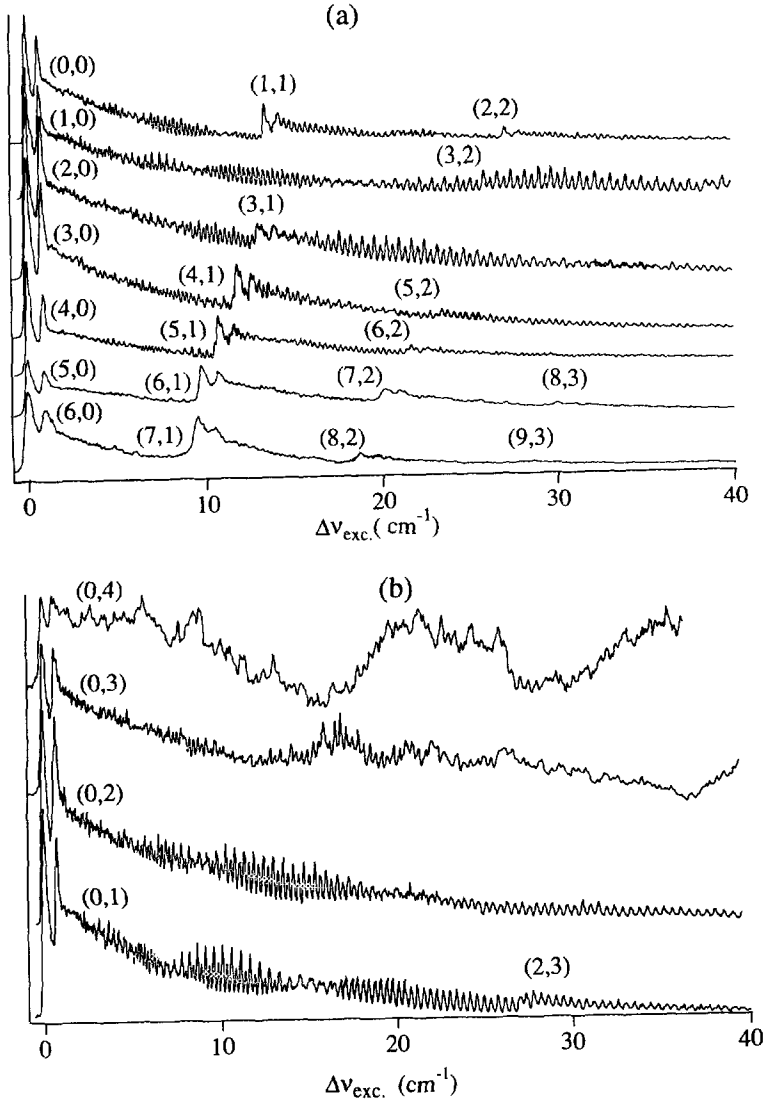

FIG. 3. Rotational contours/vibrational bands in the Dalby system, $[^2\Pi_{1/2}]_c 6s;1g \leftarrow X$: relative intensities vs relative excitation frequencies. (v', v'') assignments are indicated (a) for (v', v''), $v' = 0$–6, $v'' \leq v'$, and (b) for (v', v''), $v'' > v'$. Spectra for (0, 4) and (0, 3) bands were recorded in one scan each, while others were obtained by two or more partly overlapping scans.

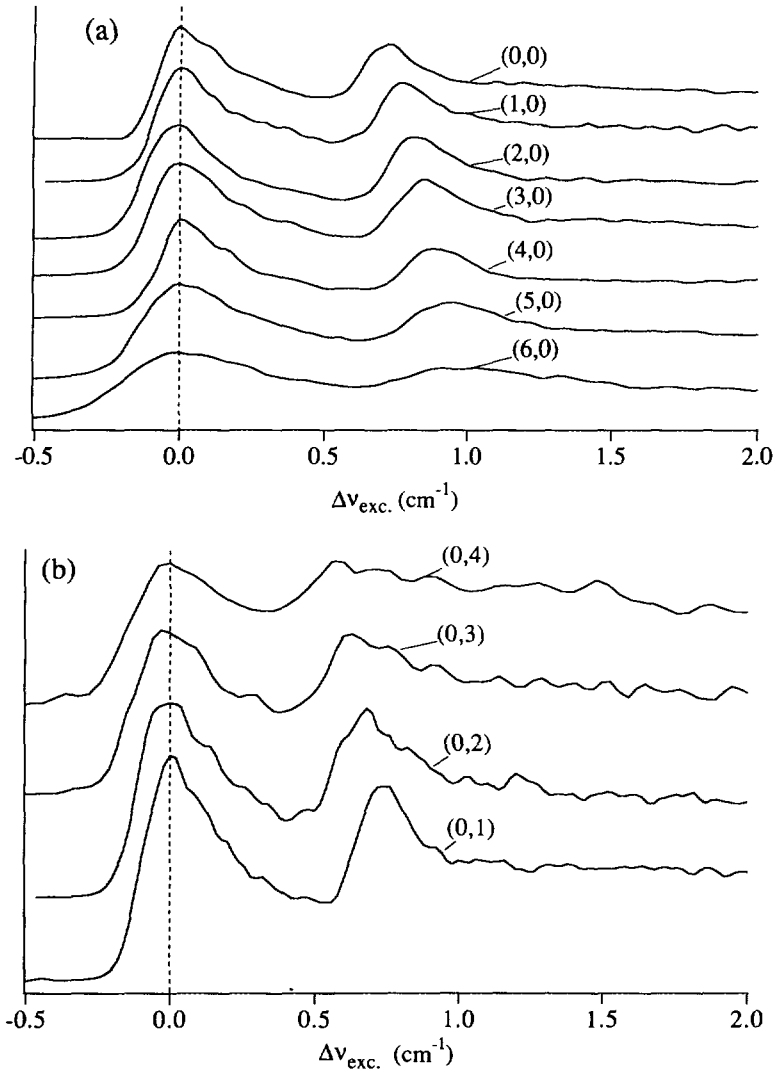

FIG. 4. Bandheads of (v', v'') bands in the Dalby system, $[^2\Pi_{1/2}]_c 6s;1g \leftarrow X$: relative intensities vs relative excitation frequencies (a) for (v', $v'' = 0$), $v' = 0$–6 and (b) for ($v' = 0$, v''), $v'' = 1$–4.

in the tail of each band. The contribution from the Q series is found to be negligible, however (*19*). Positions of the O head peaks (i.e., the peaks at the short wavenumber edges of each band) are presented in Table I along with the spacings between the O and the P peaks.

(b) The Method of Simulation Calculations

Rotational constants for vibrational levels in the excited Rydberg state ($[^2\Pi_{1/2}]_c 6s;1g$) were obtained from the data by spectral simulations.

The simulations involved calculations of relative intensities and resonance frequencies for all rotational transitions of concern. The rotational lines were displayed

TABLE I

O Bandhead Positions (a) and Spacing between *O* and *P* Bandheads ($\Delta(OP)$) (b) for (v', v'') Bands in the Dalby System

a) O band heads / cm^{-1}

$v' \backslash v''$	0	1	2	3	4
0	26785.37	26678.78	26572.71	26468.16	26363.64
1	26906.16	26800.14			
2	27025.32	(26919.58)	26813.70	26708.52	
3	27144.41	27037.96	26932.46		
4	27263.22	27156.20			
5	27381.16	27274.52	27168.6		
6	27497.69	27390.98	27285.4		
7		27506.86	27401.6		
8			27516.5	27411.3	

b) Δ(OP) / cm^{-1}

$v' \backslash v''$	0	1	2	3	4
0	0.74 ± 0.01	0.74 ± 0.01	0.68 ± 0.01	0.66	0.64
1	0.78 ± 0.01	0.80 ± 0.02			
2	0.81 ± 0.02	0.82 ± 0.02	0.84 ± 0.05		
3	0.84 ± 0.02	0.84 ± 0.10	0.86 ± 0.08		
4	0.88 ± 0.01	0.86 ± 0.07			
5	0.94 ± 0.01	0.90 ± 0.03	0.9 ± 0.2		
6	1.02 ± 0.02	0.98 ± 0.02	0.9 ± 0.2		
7		0.96 ± 0.02	1.0 ± 0.2		

as Gaussian-shaped functions which were summed up to obtain the calculated spectrum. Values for rotational constants for the upper state and linewidths were varied until satisfactory fits of experimental and calculated spectra were obtained.

Wavenumber positions of rotational lines due to $J', v' \leftarrow J'', v''$ transitions ($\nu_{exc}(J', v' \leftarrow J'', v'')$) are

$$\nu_{exc}(J', v' \leftarrow J'', v'') = (\Delta E^0_{v',v''} + \Delta E_{J'J''})/2, \tag{2}$$

where $\Delta E^0_{v',v''}$ is the spacing between the vibrational levels in the Rydberg state (v') and in the ground state (v''), in wavenumbers, and $\Delta E_{J'J''}$ is the difference between the rotational energies (in cm^{-1}) in the two states ($\Delta E_{J'J''} = E_{J'} - E_{J''}$). Calculated spectra were plotted against relative frequency ($\Delta\nu_{exc}$) equal to $\Delta E_{J'J''}/2$. Rotational energies (E_J) were expressed as the sum of two terms

$$E_J = BJ(J+1) - DJ^2(J+1)^2, \tag{3}$$

where B and D are the first- and second-order rotational constants, respectively. Thus $\Delta E_{J'J''}$ could be expressed as

$$\Delta E_{J'J''} = (J + \Delta J)(J + \Delta J + 1)B' - (J + \Delta J)^2 \times (J + \Delta J + 1)^2 D' - J(J+1)B'' + J^2(J+1)^2 D'', \tag{4}$$

where B', D' and B'', D'' are the rotational constants for the upper and the lower states, respectively. $J = J''$ and $\Delta J\,(= J' - J'')$ is -2, -1, 0, $+1$, and $+2$ for the O, P, Q, R, and S series, respectively.

Relative intensities I_{rel}, for J', $v' \leftarrow J''$, v'' transitions can simply be expressed as (*19*)

$$I_{rel} = C_{v',v''} g_{J''} S_{J',J''} \exp(-E_{J''} hc/kT), \tag{5}$$

where $E_{J''}$ is the rotational energy (in cm^{-1}) for rotational levels in the ground state, J'', $S_{J',J''}$ is the two-photon transition strength, and $g_{J''}$ is the degeneracy factor for J''. More specifically $C_{v',v''}$ can be expressed as (*3*)

$$C_{v',v''} = KF(v', v'')P^n\sigma(v'); \tag{6}$$

i.e., it is proportional to the Franck–Condon factor for the transition $v' \leftarrow v''$, ($F(v', v'')$) and a factor, $\sigma(v')$, which accounts for possible variations in the efficiency of photoionization from the excited state. Furthermore, $C_{v',v''}$ depends on the laser power (P; see Fig. 1) as P^n, where $n \leqslant 3$. K is an additional parameter dependent on the electronic structure of the molecule, geometrical factors and sample concentration. Here $C_{v',v''}$ is assumed to be independent of J' and J''.

The rotational lines calculated as described above were displayed as Gaussian-shaped functions of frequency (ν/cm^{-1}; $I(\nu)$) for a chosen bandwidth (bw/cm^{-1})

$$I(\nu) = I_{rel} \exp\left(\frac{4 \ln(2)}{bw^2} (\nu - \Delta E_{J'J''})^2\right) \tag{7}$$

assumed to be common to all rotational lines in the same vibrational band.

Rotational constants $B_{v''}$ and $D_{v''}$ used for the ground state vibrational levels, $v'' = 0$–4, were evaluated from (*22*)

$$B_v = B_e - \alpha_e(v + 1/2) \tag{8}$$

and

$$D_v = 4B_v^3/\omega_e^2 \tag{9}$$

based on B_e, α_e, and ω_e values listed by Hüber and Herzberg (*23*) or values derived by LeRoy (*24*) and Gerstenkorn *et al.* (*25*) (see Table II).

The linestrength, $S_{J',J''}$, is that part of the transition dipole moment for the two-photon transition that depends on J'' and J'. It is analogous to the Hönl–London

TABLE II

First- and Second-Order Rotational Constants for Vibrational Levels in the Ground State of Iodine Used in Spectral Analyses

v'	$B_{v''}$ a)	$D_{v''}$ b)
0	0.0373135	4.550×10^{-9}
1	0.0372013	4.476×10^{-9}
2	0.0370875	4.435×10^{-9}
3	0.0369737	4.394×10^{-9}
4	0.0368599	4.354×10^{-9}

a) $B_{v''}$ evaluated from equation (8); ref. (23)

b) $D_{v''}$ for $v'' = 1$ - 4 evaluated by equation (9); ref. (23); $D_{v''=0}$ from ref (24) and ref. (25).

factors in one-photon absorption (*22*). The functional forms of the linestrengths have been developed by Bray and Hochstrasser for the different line series (*O–S*) for $\Delta\Omega = 0$, 1, and 2 (*14*) (note the correction made by Ogorzalek Loo *et al.* in Ref. (*26*). Comparison of the shape of bandheads of calculated and observed spectra verified that the Dalby system corresponds to a $\Delta\Omega = 1$ resonance transition, in agreement with earlier findings (*3*). Characteristically $\Delta\Omega = 1$ transitions display a weak *Q* branch whose linestrength decreases rapidly with increasing *J*, while the relative intensity of other series are nearly equal (i.e., $O:P:Q:R:S \sim 1:1:0:1:1$). The same functional forms of *J* are found with both linearly and circularly polarized light.

The degeneracy factor $g_{J''}$ consists of a product of the general degeneracy factor for a diatomic rotor, $(2J'' + 1)$, and a nuclear statistics factor, $g_N(J'')$. The iodine atom nuclei are fermions with nuclear spin quantum numbers 5/2. According to the Pauli principle, therefore, when the two identical nuclei of the molecule are interchanged the total wavefunction changes sign. Only the signs of the rotational wavefunctions and the wavefunctions representing the two spin $\frac{5}{2}$ nuclei need to be considered in this context. Since the ground state of iodine is an 0_g^+ state (alternatively $^1\Sigma_g^+$), odd J'' levels are antisymmetric and even J'' levels are symmetric (*22*). Nuclear wavefunctions with even total nuclear spins (T) are antisymmetric, but those with odd total nuclear spins are symmetric. Therefore odd T combines with odd J'' quantum numbers, but even T combines with even J''. The statistical weight of nuclear states depends on T as $2T + 1$, hence the relative degeneracy is odd T:even T = odd J'':even J'' = 7:5.

The simulation procedure was based on varying the rotational parameters, $B_{v'}$ and $D_{v'}$, as well as the bandwidth for rotational lines (bw) until a satisfactory fit was obtained. $B_{v'}$ could be estimated from the spacing between the *O* and the *P* heads as described below. While $D_{v'}$ could be evaluated from $B_{v'}$ (and ω_e') by the approximation equation (Eq. (9)), a slight deviation from that relationship was normally allowed in the fit procedure.

Figure 5 shows a calculated spectrum for spectroscopic parameters obtained by simulating the (1, 0) band (see also Fig. 9 below). The rotational lines for the different rotational series are plotted underneath the calculated spectrum. Figure 6 shows the calculations for the narrow regions indicated in Fig. 5. Clearly the two peaks in the bandhead are made of overlapping *O* and *P* rotational lines. The observed rotational peaks are actually made of overlapping rotational lines which belong to the *O*, *P*, *R*, and *S* series (*Q* being negligible), and the regular alteration in intensities of neighbor peaks is found to be based on the relative contributions of rotational lines for odd J'' and even J'', i.e., the different nuclear statistics as described above. Thus the observed peaks in region (b) in Figs. 5 and 6 are made of near equal contributions of odd and even J'' rotational lines, while in regions (a) and (c) odd J'' rotational lines make the dominant contribution to the more intense peaks, but even J'' lines mainly contribute to the less intense peaks. The characteristic beat structure is found to be due to a different degree of overlap of rotational lines in different regions of a band spectrum. Maxima in the beat structure correspond to maximum overlap of lines, while "nodes" correspond to minimum overlap (see Fig. 5).

(c) $B_{v'}$ Derived from $\Delta(OP)$

A first-order approximation value for $B_{v'}$, could be derived from the spacing between the *O* and the *P* bandheads ($\Delta(OP)$). $\Delta(OP)$ is approximately equal to the difference

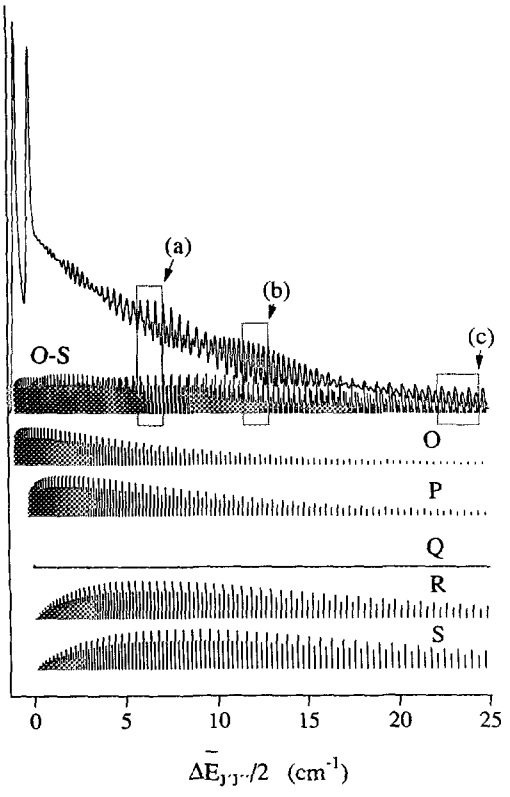

FIG. 5. Calculated rotational contour (top) and rotational lines, *O–S* (below), for $\Delta\Omega = 1$; Boltzmann distribution for 25°C; statistical weight ratio, odd J'':even $J'' = 7{:}5$; rotational constants $B'' = 0.0373135$ cm^{-1}, $D'' = 4.550 \times 10^{-9}$ cm^{-1} (corresponding to the ground state rotational constants $B_{v''=0}$ and $D_{v''=0}$; see Table II) and $B' = 0.04020$ cm^{-1}, $D' = 4.5 \times 10^{-9}$ cm^{-1} (corresponding to $B_{v'=1}$ and $D_{v'=1}$; see Fig. 9 and Table III); and a bandwidth of rotational lines of 0.16 cm^{-1}. Boxed-in areas marked (a)–(c) are blown up in Fig. 6. See definition of the *x*-axis scale ($\Delta E_{J'J''}/2$) in the text.

in wavenumber positions of the rotational lines with minimum $\Delta E_{J'J''}$ values in the *O* and *P* series (i.e., of the rotational lines for which J'' values are labeled $J_O^{\min}$ and $J_P^{\min}$, respectively; see below). By representing the rotational energies without the centrifugal term ($D = 0$ in Eq. (3)) the corresponding expressions for $\Delta E_{J'J''}$ for the *O* and the *P* series ($\Delta J = -2$ and -1; see analogous Eq. (4)) can be differentiated to derive the simple expressions

$$J_O^{\min} = \frac{3B' + B''}{2(B' - B'')} \tag{10}$$

$$J_P^{\min} = \frac{B' + B''}{2(B' - B'')}. \tag{11}$$

By substituting these into $\Delta E_{J'J''}$ (Eq. (4)) and evaluating the difference, $\Delta(OP)$ could be estimated as

$$\Delta(OP) = \frac{3B'B''}{2(B' - B'')}. \tag{12}$$

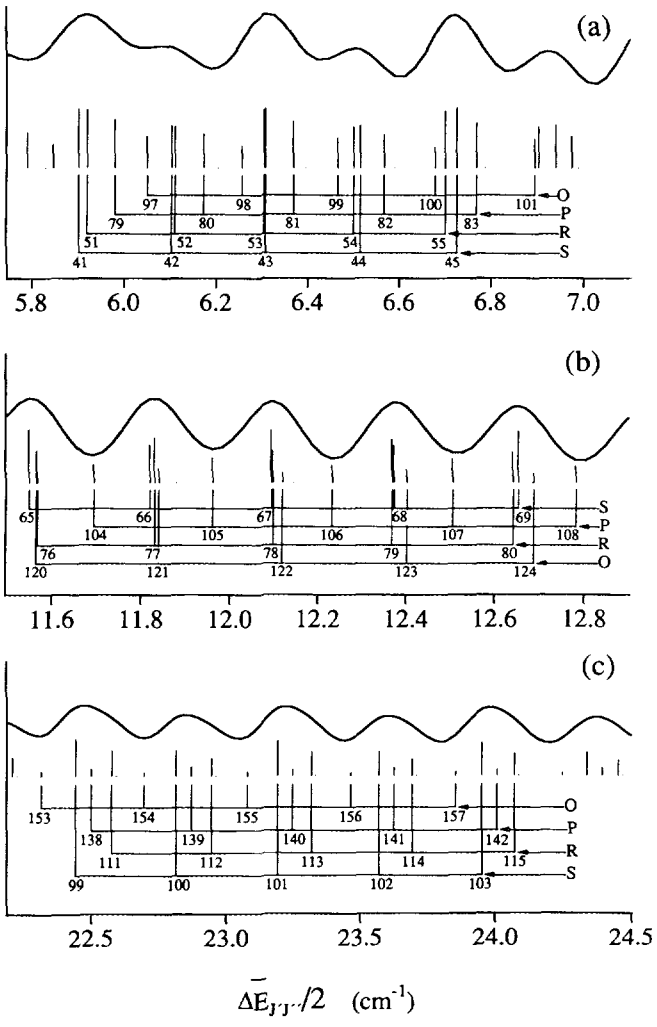

FIG. 6. Calculated REMPI spectra (top) and rotational lines (below) corresponding to the boxed-in areas in Fig. 5. See the legend to Fig. 5 for further information. Rotational line numbers are J'' values. See definition of the x-axis scale ($\Delta\bar{E}_{J'J''}/2$) in the text.

Rewriting the expression in terms of B' gives

$$B' = \frac{2\Delta(OP)B''}{2\Delta(OP) - 3B''}. \tag{13}$$

B' thus derived from $\Delta(OP)$ and known B'' constants either served as first-order approximation values in the simulation procedure or gave the final values in cases where insignificant fine rotational structure could be detected, such as for weak signals or due to overlapping bands.

(d) Simulation Calculations

Figure 7 shows calculated spectra for spectroscopic parameters as indicated. Figure 7a shows how the bandhead shape/spacing between O and P heads changes with B'

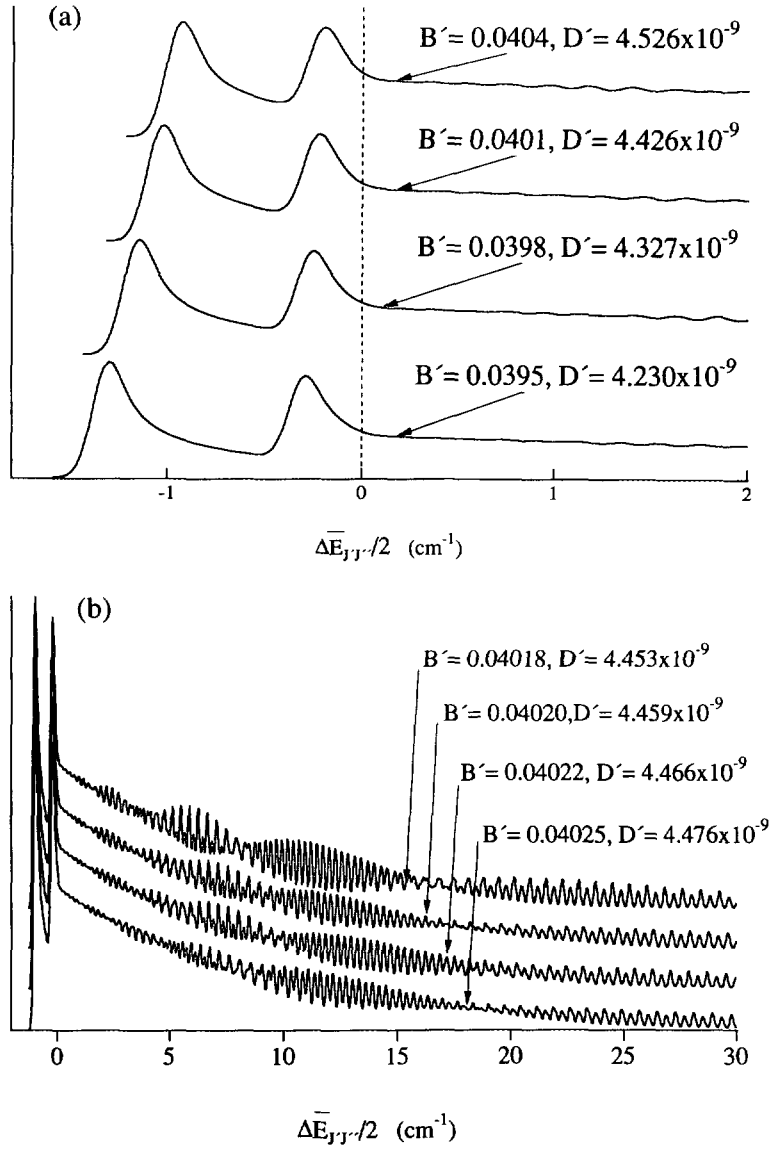

FIG. 7. Calculated bandheads (a) and rotational contours (b) for different rotational constants; B' (cm^{-1}) and corresponding D' (cm^{-1}) evaluated from Eq. (9). Other parameters used in the calculations are the same as those mentioned in the legend to Fig. 5. See definition of the x-axis scale ($\Delta E_{J'J''}/2$) in the text.

constants (for D' evaluated by Eq. (9)). The $\Delta(OP)$ values derived from such calculations were found to be in close agreement with the simple expression derived above (Eq. (12)). Figure 7b shows the effect of making slight changes to B', small enough such that insignificant variation in $\Delta(OP)$ occurs. Clearly the rotational structure is strongly dependent on small changes in the rotational constants, hence overall shape/rotational contour simulations are suitable for evaluating accurate rotational constants. The effect of varying the rotational line bandwidth is demonstrated in Fig. 8.

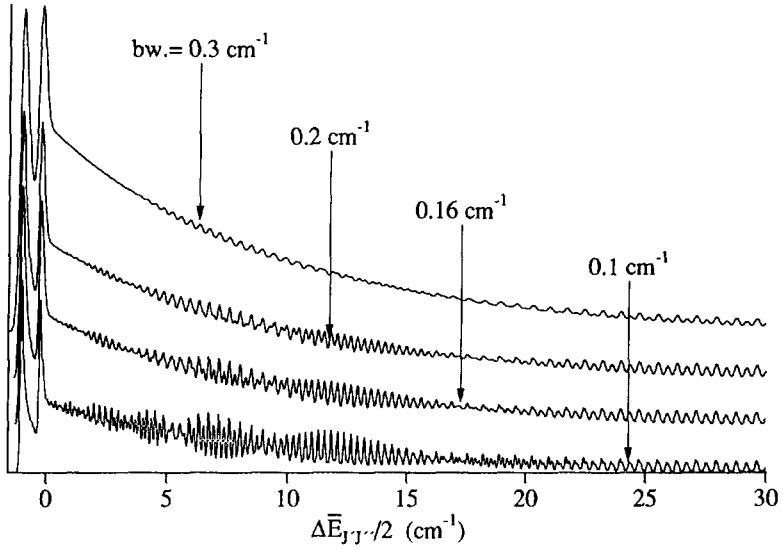

FIG. 8. Calculated rotational contours for different rotational line bandwidths (bw) as indicated. Other parameters are the same as those mentioned in the legend to Fig. 5. See definition of the x-axis scale ($\Delta E_{J'J''}/2$) in the text.

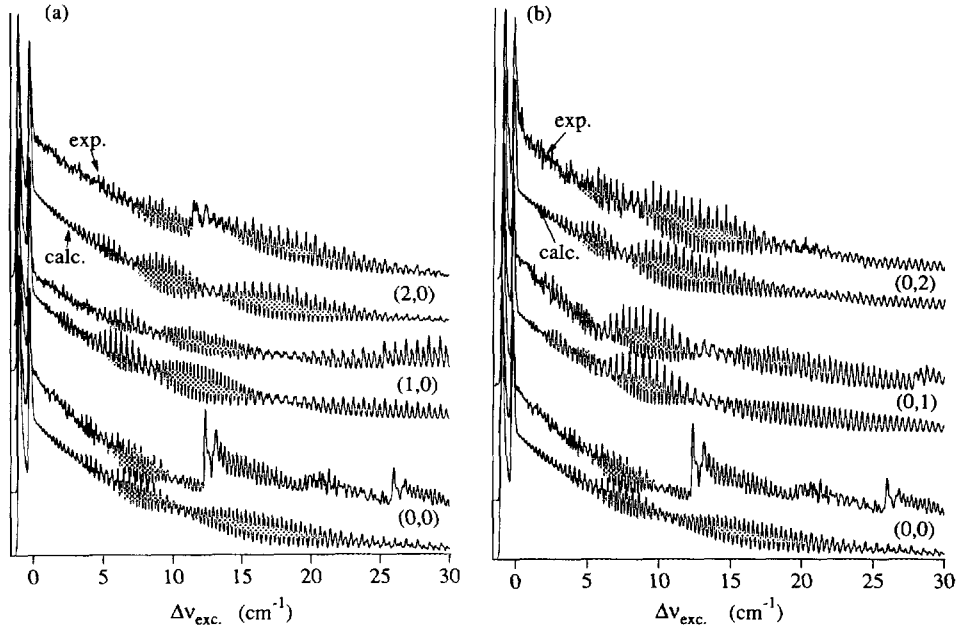

FIG. 9. Observed (top) and calculated (below) rotational contours for the (2 + 1) REMPI spectra for the Dalby system, $[^2\Pi_{1/2}]_c 6s;1g \leftarrow X$, (a) for ($v'$, $v'' = 0$), $v' = 0, 1, 2$ and (b) for ($v' = 0$, v''), $v'' = 0, 1, 2$. The x-axis scale ($\Delta\nu_{exc}$) equals $\Delta E_{J'J''}/2$ (see definition in text). Bandwidths of rotational lines in calculated spectra are 0.16 cm^{-1}.

Figure 9 shows simulations of several rotational contours. Line bandwidths were found to be about 0.16 cm^{-1} in all cases. Rotational constants are listed in Table III along with average internuclear distance values, $r_{v'}$, evaluated from the expression

$$r_{v'} = \sqrt{\frac{h}{B_{v'} 8\pi^2 c\mu}}, \tag{14}$$

which holds for a rigid rotor. μ is the reduced mass, c is the speed of light, and h is Planck's constant. Furthermore, the equilibrium values, B_e and α_e, were evaluated from the slope and intercept of a best straight line fit through a plot of $B_{v'}$ vs $v' + 0.5$, shown in Fig. 10 (Eq. (8)). These, as well as the corresponding average internuclear distance, r_e, were found to be $B_e = 0.04036 \pm 0.00001$ cm^{-1}, $\alpha_e = (1.12 \pm 0.02) \times 10^{-4}$ cm^{-1}, and $r_e = 2.5656 \pm 0.0005$ Å.

(e) Vibrational Analyses

The above described rotational analyses allow determination of the vibrational band origins ($\nu^0_{exc}(v', v'')$) as

$$\nu^0_{exc}(v', v'') = \nu_{exc}(O) + \Delta E_{J'J''}(O)/2, \tag{15}$$

where $\Delta E_{J'J''}(O)$ is the wavenumber value for an O bandhead peak derived from the calculated spectrum. $\nu_{exc}(O)$ is the position of an O bandhead peak according to the experimental spectrum (Table I). $\nu^0_{exc}(v', v'')$ values for bands where insignificant overlap occurs near the bandhead region are listed in Table IV. $\nu^0_{exc}(v', v'')$ can be expressed as

TABLE III

Rotational Constants ($B_{v'}$ and $D_{v'}$) and Internuclear Distances, $r_{v'}$, for Vibrational States (v') of the Rydberg State $[^2\Pi_{1/2}]6s$; 1g Derived from Analyses of (v', v'') Bands

(υ',υ'')	$B_{\upsilon'}$/cm^{-1}	$D_{\upsilon'}$/cm^{-1}	$r_{\upsilon'}$/Å
(0,0)/(0,1)/(0,2)	0.04030 ±0.00003	(3.1±1.5) x10^{-9}	2.568 ±0.001
(1,0)	0.04020 ±0.00005	(4.5±1.5) x10^{-9}	2.571 ±0.002
(2,0)	0.04010 ±0.00002	(3.5±2.0) x10^{-9}	2.574 ±0.001
(3,0)	0.03996 ±0.00004	(3.5±2.0) x10^{-9}	2.579 ±0.002
(4,0)	0.03985 ±0.00008	(4.8±2.0) x10^{-9}	2.582 ±0.003
(5,0)	0.03973 ±0.00010		2.586 ±0.003
(6,0)	0.03965 ±0.00010		2.588 ±0.003

a) Values derived from bands (υ',υ''); υ'= 0-4, were obtained by simulation calculations, while those derived for υ'= 5 and 6 were obtained from Δ(OP) (see text).

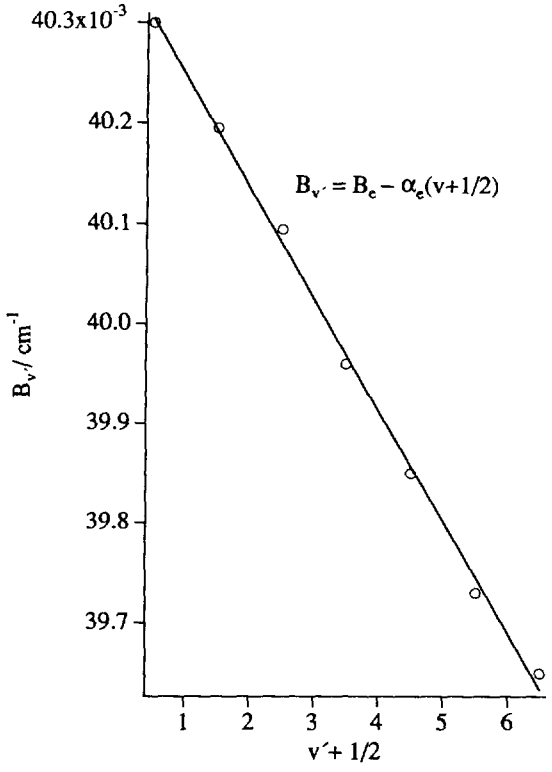

FIG. 10. Rotational constants for vibrational energy levels (v') in the $[^2\Pi_{1/2}]_e 6s;1g$ state ($B_{v'}$) plotted vs $v' + 1/2$ (data points and line fit).

$$2\nu^0_{\text{exc.}}(v', v'') = C_{v''} + \omega'_e(v' + 1/2) - \omega_e x'_e(v' + 1/2)^2, \qquad (16)$$

where $C_{v''}$ is dependent on v''. Thus the vibrational frequency (ω'_e) and the anharmonicity constant ($\omega_e x'_e$) were derived from least-squares fit analyses of the data points in Table IV as $\omega'_e = 241.8 \pm 0.5$ cm^{-1} and $\omega_e x'_e = 0.64 \pm 0.07$ cm^{-1}.

TABLE IV

Vibrational Band Origins, ν^0_{exc} (cm^{-1})

(v',v'')	$\nu^0_{\text{exc.}}$ (cm^{-1})
0,2	26573.99
0,1	26680.12
0,0	26786,91
1,0	26907.31
2,0	27026.49
3,0	27145.48
4,0	27264.57
5,0	27382.16
6,0	27498,72

DISCUSSION

(a) Rotational Analysis

Although iodine is one of the most extensively studied diatomic molecules in terms of spectroscopy, only limited rotational analyses of its Rydberg states have been done. In standard absorption spectroscopy Rydberg transition spectra appear in the VUV region between 125 and 180 nm (*1, 27*). Even though spectra have been recorded with a 10-m spectrograph (*1*) rotational structure is still largely unresolved and all the available measurements refer to bandheads and vibrational analyses. The only rotational structure or contour analyses for Rydberg states of iodine which have been reported are based on multiphoton excitation and ionization studies (*3, 8, 19, 28, 29*). Within experimental error the rotational contour for the (0, 0) band reported here (Fig. 3a) looks identical to that reported by Donovan *et al.* (Fig. 6a in Ref. (*10*)). Since our spectrum was recorded at a higher resolution (laser bandwidth about 0.05 cm^{-1} compared to 0.2 cm^{-1}) this might suggest that the resolution limit has been reached. The relatively large bandwidth of the rotational lines (0.16 cm^{-1}) could be because of a short lifetime of the Rydberg state due to rapid predissociation via repulsive states (*1, 8, 17, 27*). Rotational constants for $v' = 0$ of the $[^2\Pi_{1/2}]_c 6s;1g$ state obtained by a previous rotational analyses of the (0, 1) band of the Dalby system (*19*) agree with our more careful analyses of the same band as well as the (0, 0) and (0, 2) bands. Dalby *et al.* estimated the difference in the internuclear distances between the ground state and the excited state ($[^2\Pi_{1/2}]_c 6s;1g$), Δ, from comparison of intensities of the vibrational bands and calculated Franck–Condon factors (*3*). Thus $\Delta = (0.0988 \pm 0.002)$ Å, $r'_e = (2.568 \pm 0.002)$ Å, and $B'_e = (0.040289 \pm 0.000063)$ cm^{-1} were obtained, in very good agreement with our results. Hoy *et al.* performed analyses of rotationally resolved bands observed in a two-stage three-photon resonance excitation to a higher lying Rydberg state ($T_e = 61\,665.15$ cm^{-1}) (*29*). It was assigned as $R0_u^+$ with the most probable electronic configuration being $[^2\Pi_{1/2g}]_c 6p\sigma_u$, and rotational constants $B_e = 0.03842$ cm^{-1} and $\alpha_e = 1.6 \times 10^{-4}$ cm^{-1}. This corresponds to $r_e = 2.63$ Å, which is a significantly larger value than that obtained for the $[^2\Pi_{1/2}]_c 6s;1g$ state. Franck–Condon factor analyses of vibrationally resolved excitation functions for ion-pair ($I^+ + I^-$) formation resulted in estimates of r_e values for three ungerade Rydberg states close to the first ionization limit (*10*). Also these were found to be significantly larger than that found for the $[^2\Pi_{1/2}]_c 6s;1g$ state; i.e., $r_e = 2.60$, 2.58, and 2.58 Å for $[^2\Pi_{3/2}]_c np\pi;n = 9(\nu_{00} = 72\,460\ cm^{-1})$, $10(\nu_{00} = 73\,100\ cm^{-1})$, and $11(\nu_{00} = 73\,640\ cm^{-1})$, respectively.

(b) Vibrational Analyses

The frequency, ω_e, and the anharmonicity constant, $\omega_e x_e$, for $[^2\Pi_{1/2}]_c 6s;1g$, were derived from evaluation of band origins, based on the rotational analyses as described above. These are found to be in good agreement with those obtained by Dalby *et al.* ($\omega_e = (241.41 \pm 0.04)$ cm^{-1} and $\omega_e x_e = (0.58 \pm 0.36)$ cm^{-1}), based on bandhead analyses (*3*). The vibrational frequency of this state is about 13% higher than that of the ground state. Larger frequencies are to be expected for a Rydberg system due to the promotion of a weakly antibonding electron to a diffuse Rydberg orbital. Venkateswarlu (*1*) found ω_o for ungerade Rydberg states, according to absorption spectra, to be between 190 and 284 cm^{-1}, compared to 213.3 cm^{-1} for the ground state ($\omega_e = 214.502$ cm^{-1}; $\omega_e x_e = 0.6147$ cm^{-1} (*23*)). On average ω_o was found to be about 230 cm^{-1} or about 8% larger than that for the ground state. Donovan *et al.* found the

vibrational frequency of the gerade Rydberg state to be about 10% larger than that of the ground state (*8*). For $R0_u^+$, ω_e and $\omega_e x_e$ values are close to those found for the ground state (ω_e = 209.29 cm^{-1}; $\omega_e x_e$ = 0.859 cm^{-1}) (*30*). Estimated ω_e values for the $[^2\Pi_{3/2}]_c np\pi$ states (n = 9, 10, and 11) are ω_e = 210.5, 229, and 229 cm^{-1}, respectively (*10*).

CONCLUSION

Rotational contours for (2 + 1) REMPI spectra of iodine due to the resonance transition $[^2\Pi_{1/2}]_c 6s;1g \leftarrow X$ have been recorded and analyzed by simulation calculations. The spectra can be simulated by assuming that the energies of the rotational levels involved can be formulated in the simple form $E(J) = BJ(J + 1) - DJ^2(J + 1)^2$. Furthermore intensities could be reproduced by using explicit forms of linestrengths determined by Bray and Hochstrasser for $\Delta\Omega = 1$ transitions and the statistical weight ratio, odd J'':even J'' = 7:5, in accordance with the total nuclear spin statistics. No indication of a rotational perturbation is found in contrast with findings for many other Rydberg systems (*1, 8, 30*). The simulation calculations allowed evaluations of rotational constants, internuclear distance values, and vibrational parameters based on evaluations of band origins.

ACKNOWLEDGMENTS

We are grateful for financial support from the Icelandic Science Foundation and from the Research Foundation of the University of Iceland. We are also grateful for useful discussions with and comments from our colleagues R. J. Donovan, K. P. Lawley, and T. Ridley at the University of Edinburgh, and A. J. Yencha, State University of New York at Albany.

RECEIVED: August 18, 1993

REFERENCES

1. P. VENKATESWARLU, *Can. J. Phys.* **48,** 1055–1080 (1970).
2. G. PETTY, C. TAI, AND F. W. DALBY, *Phys. Rev. Lett.* **34,** 1207–1209 (1975).
3. F. W. DALBY, G. PETTY-SIL, M. H. PRYCE, AND C. TAI, *Can. J. Phys.* **55,** 1033–1046 (1977).
4. K. K. LEHMANN, J. SMOLAREK, AND L. GOODMAN, *J. Chem. Phys.* **69,** 1569–1573 (1978).
5. J. C. MILLER, *J. Phys. Chem.* **91,** 2589–2592 (1987).
6. M. WU AND P. M. JOHNSON, *J. Chem. Phys.* **90,** 74–80 (1989).
7. R. R. DASARI AND F. W. DALBY, *J. Chem. Phys.* **92,** 3984–3986 (1990).
8. R. J. DONOVAN, R. V. FLOOD, K. P. LAWLEY, A. J. YENCHA, AND T. RIDLEY, *Chem. Phys.* **164,** 439–450 (1992).
9. B. R. HIGGINSON, D. R. LLOYD, AND P. J. ROBERTS, *Chem. Phys. Lett.* **19,** 480–482 (1973).
10. Á. KVARAN, A. J. YENCHA, D. K. KELA, R. J. DONOVAN, AND A. HOPKIRK, *Chem. Phys. Lett.* **179,** 263–267 (1991).
11. K. P. LAWLEY, R. J. DONOVAN, T. RIDLEY, A. J. YENCHA, AND T. ICHIMURA, *Chem. Phys. Lett.* **168,** 168–172 (1990).
12. T. RIDLEY, K. P. LAWLEY, R. J. DONOVAN, AND A. J. YENCHA, *Chem. Phys.* **148,** 315–323 (1990).
13. W. M. MCCLAIN, *J. Chem. Phys.* **55,** 2789–2796 (1971).
14. R. G. BRAY AND R. M. HOCHSTRASSER, *Mol. Phys.* **31,** 1199–1211 (1976).
15. L. ZANDEE, R. B. BERNSTEIN, and D. A. LICHTIN, *J. Chem. Phys.* **69,** 3427–3429 (1978).
16. C. TAI AND F. W. DALBY, *Can. J. Phys.* **56,** 183–190 (1978).
17. R. J. DONOVAN, B. V. O'GRADY, K. SHOBATAKE, AND A. HIRAYA, *Chem. Phys. Lett.* **122,** 612–616 (1985).
18. M. S. DEVRIES, N. J. A. VAN VEEN, T. BALLER, AND A. E. DEVRIES, *Chem. Phys.* **56,** 157–165 (1981).
19. WANG HUASHENG, J. ÁSGEIRSSON, Á. KVARAN, R. J. DONOVAN, R. V. FLOOD, K. P. LAWLEY, T. RIDLEY, AND A. J. YENCHA, *J. Mol. Struct.* **293,** 217–222 (1993).

20. T. E. ADAMS, R. J. S. MORRISON, AND E. R. GRANT, *Rev. Sci. Instrum.* **51,** 141–142 (1980).
21. C. E. MOORE, "Atomic Energy Levels," Vol. 2, p. 467, National Bureau of Standards, Washington, DC, 1971.
22. G. HERZBERG, "Spectra of Diatomic Molecules," Van Nostrand–Reinhold, New York, 1950.
23. K. P. HÜBER AND G. HERZBERG, "Constants of Diatomic Molecules," Van Nostrand–Reinhold, New York, 1979.
24. R. J. LEROY, *J. Chem. Phys.* **52,** 2683–2689 (1970).
25. S. GERSTENKORN, P. LUC, AND A. PERRIN, *J. Mol. Spectrosc.* **64,** 56–69 (1977).
26. R. OGORZALEK LOO, W. J. MARINELLI, P. L. HOUSTON, S. AREPALLI, J. R. WIESENFELD, AND R. W. FIELD, *J. Chem. Phys.* **91,** 5185–5200 (1989).
27. A. HIRAYA, K. SHOBATAKE, R. J. DONOVAN, AND A. HOPKIRK, *J. Chem. Phys.* **88,** 52–57 (1988).
28. A. D. WILLIAMSON AND R. N. COMPTON, *Chem. Phys. Lett.* **62,** 295–299 (1979).
29. A. R. HOY, S. M. JAYWANT, AND J. C. D. BRAND, *Mol. Phys.* **60,** 749–759 (1987).
30. Á. KVARAN, G. H. JÓHANNESSON, H. WANG, R. J. DONOVAN, K. P. LAWLEY, T. RIDLEY, AND A. J. YENCHA, in preparation.